A Blank Slate? Layer-by-Layer Deposition of Hyaluronic Acid and Chitosan onto Various Surfaces

Tristan I. Croll,[†] Andrea J. O'Connor,[‡] Geoffrey W. Stevens,[‡] and Justin J. Cooper-White*,[†]

Australian Institute of Bio- and Nanotechnology, University of Queensland, 4072 Australia, and Department of Chemical and Biomolecular Engineering, University of Melbourne, 3010 Australia

Received January 16, 2006; Revised Manuscript Received March 16, 2006

Although poly(α-hydroxy esters), especially the PLGA family of lactic acid/glycolic acid copolymers, have many properties which make them promising materials for tissue engineering, the inherent chemistry of surfaces made from these particular polymers is problematic. In vivo, they promote a strong foreign-body response as a result of nonspecific adsorption and denaturation of serum proteins, which generally results in the formation of a nonfunctional fibrous capsule. Surface modification post-production of the scaffolds is an often-utilized approach to solving this problem, conceptually allowing the formation of a scaffold with mechanical properties defined by the bulk material and molecular-level interactions defined by the modified surface properties. A promising concept is the so-called "blank slate": essentially a surface that is rendered resistant to nonspecific protein adsorption but can be readily activated to covalently bind bio-functional molecules such as extracellular matrix proteins, growth factors or polysaccharides. This study focuses on the use of the quartz crystal microbalance (QCM) to follow the layer-by-layer (LbL) electrostatic deposition of high molecular weight hyaluronic acid and chitosan onto PLGA surfaces rendered positively charged by aminolysis, to form a robust, protein-resistant coating. We further show that this surface may be further functionalized via the covalent attachment of collagen IV, which may then be used as a template for the self-assembly of basement membrane components from dilute Matrigel. The response of NIH-3T3 fibroblasts to these surfaces was also followed and shown to closely parallel the results observed in the QCM.

Introduction

The use of biodegradable polymers such as poly(lactic-*co*-glycolic acid) (PLGA) to form highly porous scaffolds is a well-established concept in tissue engineering. Their ease of processing, for example via thermally induced phase separation (TIPS),[1−3] allows the production of scaffolds with bulk Young's moduli ranging over at least 3 orders of magnitude, from tens of kilopascals (similar to soft tissues such as fat and muscle) to tens of megapascals (approaching that of bone), and coherent structures can be formed with porosities as high as 98%. However, the surface chemistry of most currently available polymers is a major issue hindering their widespread success when implanted. Similarly to most moderately hydrophobic surfaces, when brought into contact with bodily fluids they very quickly become coated with a layer of serum proteins via hydrophobic interactions, the denaturation of which leads to a significant foreign body response and uncontrolled fibrotic encapsulation.[4−6]

A large number of papers now exists in the literature describing the surface modification of polymers for tissue engineering purposes. Techniques described include surface entrapment modification, UV treatment, and plasma treatment.[7−12] Of these, only surface entrapment modification has shown the potential to treat three-dimensional structures of more than a few millimeters in thickness.[13,14] However, this technique requires relatively solid structures to avoid softening and collapse of the scaffold structure during treatment. By comparison, synthetic porous scaffolds for the tissue engineering of soft tissues often combine large volumes of up to hundreds of milliliters with internal structures of submicron dimensions.[1−3]

Layer-by-layer deposition has been reported in many papers as a facile technique for the modification of a wide range of surfaces.[15−18] Essentially, a polyelectrolyte is deposited from an aqueous solution onto a surface of opposite charge. This leads to a reversal of the net surface charge, due to excess charged groups on the polymer chain, allowing the subsequent deposition of a second, oppositely charged polyelectrolyte. Multiple repetitions of this process lead to the build-up of a strong, coherent surface coating, generally with a thickness ranging from tens to hundreds of nanometers.

Aminolysis, a technique widely used in the synthetic textile industry for modification of poly(ethylene terephthalate) (PET) fabrics,[19−21] has recently been recognized[22,23] as a highly versatile method to impart functionality to the surface of ester-based polymers for tissue engineering. Using multifunctional amines such as ethylenediamine, *N*-aminoethyl-1,3-propanedi-amine,[22] or branched polyethylenimine, for example, one can add a significant density of primary amine groups to the surface in the form of new polymer end groups. These impart a positive charge to the surface, crucial to the layer-by-layer technique, but also provide functionality for the convenient covalent attachment of these layers to give added strength to the multilayer-substrate bond.

Arguably the most important factor in the success or failure of a tissue engineering scaffold is the prevention of a foreign body reaction upon implantation. It has been shown in numerous situations that a significant adverse response can be avoided by creating a surface which is resistant to protein adsorption.[24−26] If this surface, however, contains functional groups which allow,

* Corresponding author. E-mail: j.cooperwhite@uq.edu.au.
† University of Queensland.
‡ University of Melbourne.

CDV

under certain conditions, the covalent attachment of proteins or functional sequences, one has what may be termed a "blank slate", a surface with no inherent interactions which may be tailored via the attachment of functional molecules specific to the tissue of interest.

In this paper, we characterize the layer-by-layer electrostatic deposition of very high molecular weight HA and chitosan on PLGA films aminolysed using low-molecular-weight polyethylenimine (PEI) in the presence or absence of the cross-linking system 1-ethyl-3-(3-dimethylaminopropyl)-carbodiimide/N-hydroxysuccinimide (EDAC/NHS).

Using the quartz crystal microbalance (QCM), the effects of cross-linking agent and polyelectrolyte concentration on layer thickness and deposition kinetics were investigated. Surfaces formed in this way were subjected to various protein challenges, and shown to be nonadhesive under physiological salt conditions. It was demonstrated that, under nonphysiological conditions, collagen IV could be covalently attached to these surfaces. This collagen IV was further used as a template for the self-assembly of basement membrane components from dilute Matrigel. Finally, the short- and long-term responses of NIH-3T3 fibroblasts to these surfaces under in vitro culture conditions were analyzed in terms of attachment, spreading, and proliferation.

Materials and Methods

Materials. Glacial acetic acid, ammonia (25% v/v), hydrogen peroxide (25% v/v), dimethyl sulfoxide (DMSO), dimethylformamide (DMF), n-hexane, methanol, toluene, and acetone were all AR grade and obtained from various sources. Dimethyl carbonate, 1-ethyl-3-(3-dimethylaminopropyl)carbodiimide (EDAC), N-hydroxysuccinimide (NHS), 1,4-diazabicyclo[2,2,2]-octane (DABCO), morpholino(ethanesulfonic acid) (MES), glycerol, hydrochloric acid, paraformaldehyde (PFA), sodium bicarbonate, sodium chloride, sodium citrate, sodium hydroxide, chlorotrimethylsilane, decanethiol, 11-mercaptoundecanoic acid, and 1-methyl-3-mercaptopropionate were obtained from Sigma-Aldrich and used as received.

Poly(D,L-lactide-co-glycolide) (PLGA) with a lactide:glycolide ratio of 75:25 was purchased from Birmingham Polymers and used as supplied. Chitosan 500 (Wako Fine Chemicals) was kindly donated by Professor Yoshinari Baba of Miyazaki University. Hyaluronic acid (HA), MW 1.6 MDa was obtained from Lifecore Biomedical. Branched polyethylenimine (PEI), MW = 1200 Da was obtained from Sigma-Aldrich.

Collagen IV (Col IV) from human placenta, human fibronectin (Fn), and bovine serum albumin (Alb) were obtained from Sigma-Aldrich. BD Full Matrigel was obtained from Becton Dickinson. Dulbecco's Modified Eagle Medium (DMEM), fetal bovine serum (FBS), phosphate buffered saline, and gentamycin sulfate (10 mg/mL) were obtained from Gibco. All tissue culture plastic (TCP) materials were Nunclon brand.

PO−PRO 3-Iodide and Alexa Fluor 488 Phalloidin were obtained from Invitrogen and handled according to the manufacturers' instructions.

QCM Analysis. Gold-coated silicon QCM electrodes (13 mm diameter; Q-Sense) were cleaned for 5 min in RCA solution (5:1:1 water:ammonia:hydrogen peroxide by volume) at 75 °C, rinsed thoroughly with water followed by ethanol, and immersed in a 5 mM solution of 1-methyl-3-mercaptopropionate in ethanol overnight to provide a surface suitable for PLGA coating. The electrodes were then spin-coated for 2 min at 3000 rpm with a 0.8% solution of PLGA in dimethyl carbonate and annealed for 2 h at approximately 75 °C on a hotplate.

Some runs were also carried out using decanethiol- and 11-mercaptoundecanoic acid-modified gold electrodes. In the case of the decanethiol substrate, a positively charged surface was obtained by adsorbing low molecular weight PEI at basic pH. The 11-mercaptoundecanoic acid surface was modified by covalently coupling ethylenediamine in the presence of EDAC and NHS.

QCM analysis took place in a Q-Sense QCM-D apparatus (27, 28). The electrodes were placed in the analysis chamber, and measurements were taken continuously at the fundamental frequency of 5 MHz, as well as the 3rd, 5th and 7th overtones (15, 25 and 35 MHz, respectively). The desired solutions were allowed to flow through the measurement chamber as required. The fundamental frequency was disregarded for further analysis, as this is often significantly affected by interactions with the crystal mount.

Analysis and modeling of layer thickness was carried out using the QTools software provided with the instrument.

Preparation of Surfaces for Cell Culture. Glass coverslips (13 mm diameter) were cleaned in a hot solution of 1 part 25% ammonia in 9 parts 30% hydrogen peroxide for 5−10 min, rinsed thoroughly with milli-Q water, and dried under vacuum. They were then rendered hydrophobic by incubating in a 5% solution of chlorotrimethylsilane (CTMS) in n-hexane and rinsed thoroughly with n-hexane followed by toluene. The hydrophobic coverslips were loaded into a custom-made Teflon rack, lowered vertically into a beaker containing a 2% solution of PLGA in dimethyl carbonate, and withdrawn at a defined rate of 2 cm/min. After approximately 2 min in the vapor space just above the solution, the coverslips were transferred into individual 15 mL BD Falcon tubes and loosely capped. Finally, these were placed in an aluminum vacuum vessel and dried overnight on a hotplate set at 90 °C, to a final vacuum of 5×10^{-3} mbar.

Coverslips were placed into individual wells in 24-well tissue culture plates, with small stainless steel rods on the bottom of each well to keep them slightly elevated and facilitate removal. These were then transferred to a biological safety cabinet and disinfected using 70% ethanol for 10 min. All further treatment steps took place within this cabinet, using filter-sterilized solutions.

The surfaces were aminolysed using 1 mL per well of a 20 mg/mL solution of PEI in water for 60 min and rinsed thoroughly with 5 mM MES, pH 5.5 (hereafter referred to as MES buffer). HA solution (50 μg/mL in MES) was mixed with 1 part in 100 of 50 mg/mL EDAC, 100 mg/mL NHS in DMF 10 min before addition to the wells (1 mL/well). After 15 min, the HA solution was removed and replaced with 2 mL of MES buffer as a rinse, followed by replacement with 1 mL of chitosan solution (50 μg/mL in MES) for 15 min, and another rinse with 2 mL of MES buffer. This process was repeated until 7 layers had been deposited (HA outermost). The final layer was incubated for 30 min rather than 15 to ensure a complete coat. These surfaces will hereafter be referred to as multilayer surfaces.

One additional set of coverslips was hydrolyzed using 0.01 M sodium hydroxide for 60 min and rinsed thoroughly with MES buffer.

Multilayer surfaces to be further functionalized via collagen IV attachment were formed directly onto the tissue culture polystyrene (TCP) surface within the plates, using the native positive charge of this surface to drive initial HA attachment. The multilayer coating process was identical to that used above for PLGA, minus the aminolysis step. The surfaces were stored in MES buffer at room temperature until further use (up to 4 days) and reactivated for covalent attachment by incubating with a 0.5 mg/mL EDAC, 1 mg/mL NHS solution in MES buffer for 30 min. Collagen IV solution (2.5 mg/mL in 0.1M acetic acid) was diluted to 50 μg/mL in MES buffer, incubated with the surfaces (200 μL/well) overnight, and rinsed with MES followed by PBS. Matrigel was thawed overnight on ice, diluted 1:20 in ice-cold DMEM, incubated with the surfaces (200 μL/well) for 2 h, and rinsed with DMEM followed by PBS.

Treated coverslips were transferred into multilayer-coated culture plates to prevent nonspecific attachment, and all surfaces were stored in 1 mL/well PBS until further use.

Cell Culture. One milliliter of NIH-3T3 fibroblasts cryopreserved in liquid N_2 at a density of 10^6/mL was thawed, suspended in 10 mL DMEM containing 10% FBS and 10 μg/mL gentamycin sulfate

CDV

(hereafter referred to as medium), pelleted and resuspended in 20 mL fresh medium, and cultured in a T-75 tissue culture plate to approximately 70–80% confluence. The cells were then trypsinized with 5 mL of trypsin-EDTA, neutralized with 5 mL of medium, counted and re-suspended at a density of 10^5/mL.

All surfaces to be cultured were rinsed with DMEM and incubated with 500 μL of media for 15 min at 37 °C in an incubator prior to seeding. The cell suspension was pipetted into each well (100 μL per well) with gentle agitation to distribute the cells, and the plates returned to the incubator. This was marked as time zero for each plate. After the desired time, the plates were rinsed with PBS, fixed using 4% PFA in PBS for 30 min, and stored in PBS in a refrigerator until analysis.

Fluorescence Microscopy. The fixed cultures were incubated with 50 μg/mL ribonuclease A in 2X SSC buffer (0.3 M NaCl, 0.03 M sodium citrate, pH 7.0) for 30 min at room temperature to remove cytoplasmic RNA. After rinsing with 2X SSC, they were then incubated with 200 μL/well of 5 U/mL Alexa Fluor 488 Phalloidin for 30 min, followed by 200 μL of 2 μM PO–PRO for a further 10 min. After rinsing with PBS, 500 μL of a 90% glycerol, 9% PBS, 1% DABCO solution was added to each well. The plates were then wrapped in aluminum foil, and stored in a refrigerator until further use.

Microscopic analysis was carried out using a Nikon TE–2000 inverted fluorescence microscope using standard FITC and rhodamine fluorescence filter cubes (Chroma) and a cooled 1.3 megapixel camera (PCO Sensicam). Five red-fluorescent images (nuclei) per well were captured using a 4× objective (6.56 mm^2/image, 18.6% of total area) for cell counting purposes, and higher-magnification composite images were captured to determine cell morphology.

Cell counting was carried out using software techniques. The images were first opened in an image editing package (Adobe Photoshop) and the grayscale levels adjusted for maximum contrast. An edge-enhancement filter (unsharp mask) was then used to selectively enhance objects on the scale of nuclei (4–10 pixels in radius). Each image was then opened in an analysis package (ImageJ, National Institutes of Health), converted to a black-and-white image using a manually set threshold, and analyzed for particles. Particles between 10 and 100 pixels in area were counted as individual cells; particles smaller than 10 pixels were assumed to be noise, while particles larger than 100 pixels were counted manually using the original image. The accuracy of this technique was estimated as better than ±5%, well above intersample variability.

Results

LbL Deposition in the Absence of Cross-Linking Agent. Layer-by-layer deposition was carried out on a PEI-coated decanethiol-modified QCM electrode using 50 μg/mL chitosan and HA in 5 mM MES buffer in the absence of EDAC and NHS. Figure 1 shows a trace of frequency and dissipation changes at the third overtone. The growing film initially builds up regularly; however, it becomes unstable with the addition of further layers. This is likely due to the formation of soluble macromolecular complexes between the previous layer and the new polymer solution, as has been observed previously with high molecular weight polyelectrolytes.[29] Upon the addition of phosphate buffered saline at pH 7.4, the majority of the film is quickly lost. This is expected, since the low pK_a of chitosan (approximately 6.1) means that most of its positive charge is lost at this pH.

LbL Buildup in the Presence of Cross-Linking Agent. LbL deposition was carried out under identical conditions to those described above, except that 10 μL of a 50 mg/mL EDAC/100 mg/mL NHS solution in DMF was added for each milliliter of HA solution 10 min before addition to the system (Figure 2). Under these conditions, the frequency and dissipation changes due to each layer were substantially higher, indicating thicker, more viscous layers.
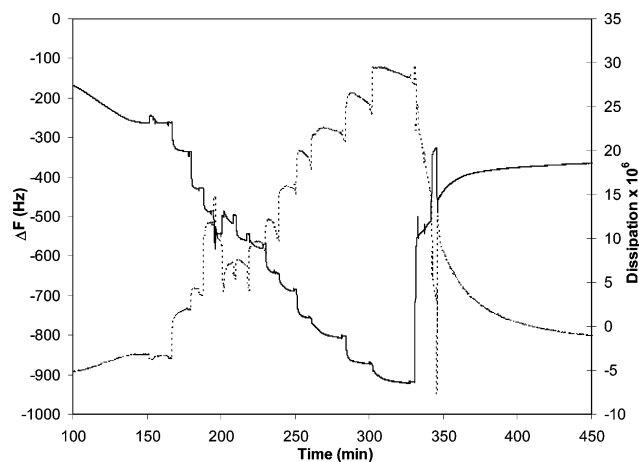
Figure 1. Frequency (solid line) and dissipation (dashed line) changes during LbL buildup in the absence of cross-linking agent. Instability is noted after the first three layers. The buffer was changed to PBS at 330 min, at which point the majority of the film was lost.
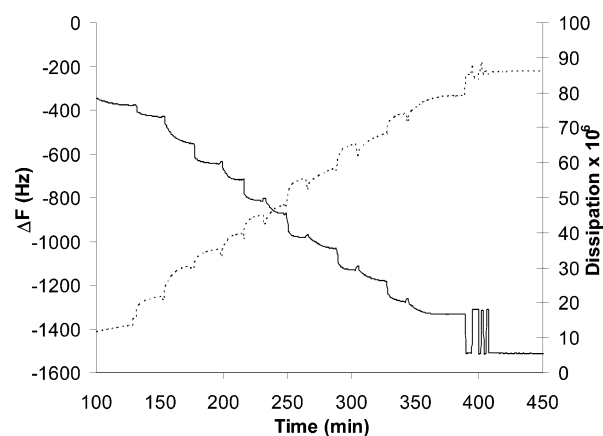
Figure 2. Frequency (solid line) and dissipation (dashed line) changes during LbL buildup in the presence of EDAC/NHS on a PEI-coated decanethiol substrate. Even layers are formed with no obvious instability. The film swells somewhat upon exposure to PBS (at t = 390), but there is no significant loss of mass over multiple cycles of PBS/MES changes.

Upon addition of PBS, the film swelled somewhat as evidenced by a drop in frequency and increase in dissipation, in stark contrast to the non-crosslinked case. Upon returning to MES buffer, the film returned to a collapsed state, with a slight increase in frequency relative to the previous equilibrium value. Upon further cycling consisting of 2 min each of PBS and MES (2 $^1/_2$ cycles), the same swelling and contraction behavior was seen; however, no further loss of mass was observed.

The average cumulative changes, after rinsing, in frequency and dissipation at the 3rd overtone as a function of layer number for four separate films are shown in Figure 3 (solid lines). After the first two layers, the frequency and dissipation changed essentially linearly with respect to the number of bilayers.

The rate of deposition of each layer was initially exponential, followed by a slow increase due to rearrangement of the surface structure. This initial deposition phase for each layer (>90% of the final layer mass) was fitted to an exponential decay curve using a least-squares algorithm, and the half-times were plotted as a function of layer number (Figure 4, solid lines).

Using the modeling software (Q-Tools) provided with the instrument, the frequency and dissipation data for four surfaces was fitted to the Voight model assuming a layer density of 1100 kg/m^3 in order to determine the film thickness.[30] The resulting
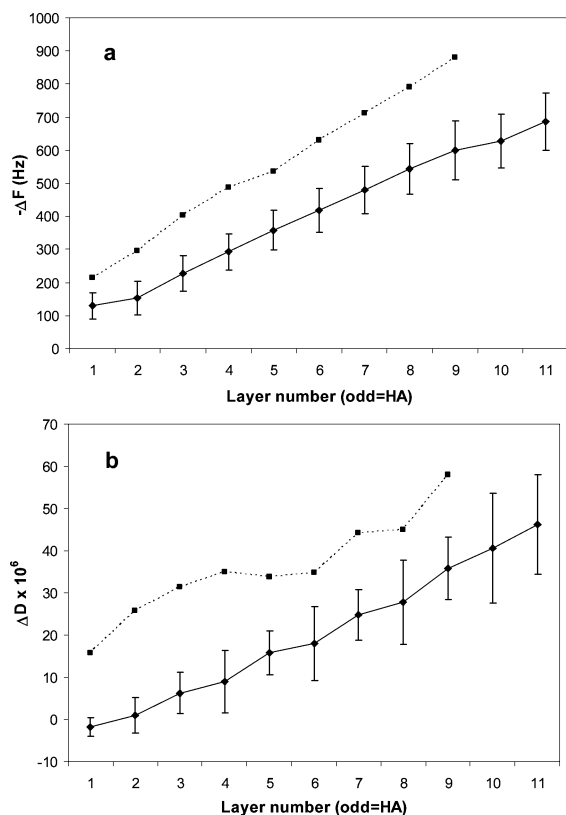
CDV

Figure 3. Cumulative changes at 15 MHz in (a) frequency and (b) dissipation as a function of number of layers deposited on a PLGA substrate from 50 μg/mL (solid lines, $n = 4$) or 500 μg/mL ($n = 1$) solutions. Error bars = 1 standard deviation.

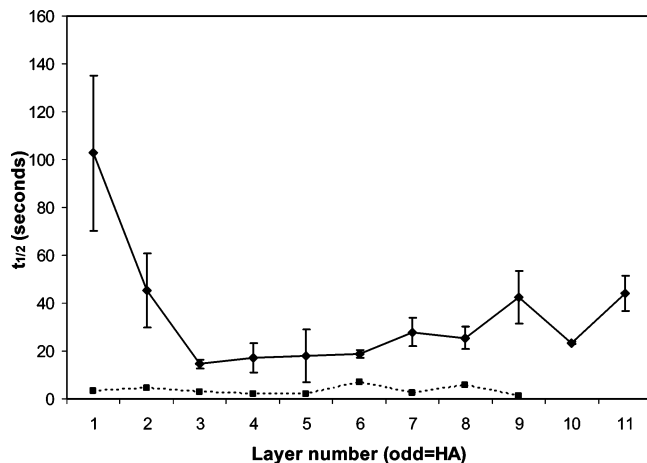**Figure 4.** Half-time of initial deposition phase from 50 μg/mL (solid line, $n = 4$) or 500 μg/mL (dashed line, $n = 1$) polymer solutions as a function of layer number. Error bars = 1 standard deviation.

thickness data is plotted in Figure 5. The film thickness was determined to increase linearly with respect to layer number, at a rate of approximately 6 nm per layer.

Effect of Polymer Concentration on Buildup. In situations where the surface/volume ratio of the material to be coated is relatively high, such as 3D scaffolds, a similarly high concentration of polymer may be required to fully coat the surface. Therefore, one film was treated at a polyelectrolyte concentration of 500 μg/mL under identical conditions to the previous films (dashed lines in Figures 3 and 4). The frequency (Figure 3a) and dissipation (Figure 3b) changes were significantly higher than those measured under low polyelectrolyte conditions. After the first four layers, the frequency change per layer settled to
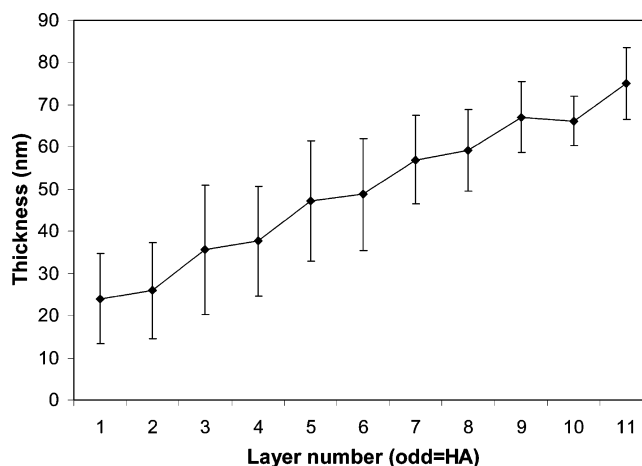

Figure 5. Thickness of the growing LbL film on a PLGA substrate at 50 μg/mL polyelectrolyte concentration calculated using the Voight model ($n = 4$). Error bars = 1 standard deviation.
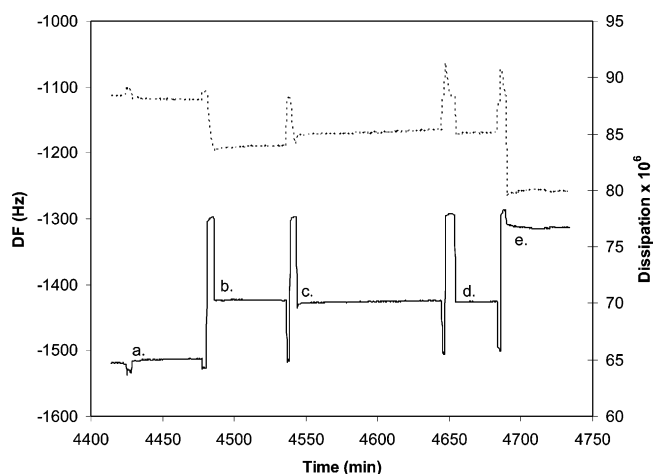

Figure 6. Frequency (solid line) and dissipation (dashed line) response to various protein challenges. (a) 5 μg/mL each Fn and Alb in PBS, pH 7.4; (b) 5 μg/mL Fn/Alb in 5 mM MES, 0.15 M NaCl, pH 5.5; (c) 5 μg/mL Fn/Alb in 5 mM MES, 0.15M NaCl, pH 5.5, EDAC/NHS; (d) 10 μg/mL Col-IV in 5 mM MES, 0.15M NaCl, EDAC/NHS; (e) 10 μg/mL Col-IV in 5 mM MES, salt-free, EDAC/NHS. Films were washed with PBS and salt-free MES between protein solutions.

approximately 30% higher than that seen under low polyelectrolyte concentrations.

The deposition kinetics under high polyelectrolyte concentration conditions (Figure 4) were extremely fast, with characteristic half-times of approximately 3−5 s. Thus >90% of the film deposition occurred during the 10−20 s required for changing solutions.

Protein Resistance. The film of Figure 2 was incubated in PBS within the QCM apparatus for 2 days before being incubated with a number of protein solutions (Figure 6). After each protein solution, the film was rinsed with PBS and salt-free MES buffer for two minutes each. No significant change in frequency was observed upon incubation with a mixture of 5 μg/mL each of Fn and Alb either in PBS or in MES buffer containing 0.15 M salt, in the presence or absence of EDAC/NHS (a, b, and c, respectively). A solution containing 10 μg/mL col-IV in MES buffer with 0.15 M salt and EDAC/NHS similarly caused no significant change. However, a significant drop in frequency coupled with a large drop in dissipation was observed upon incubation of the film with 10 μg/mL col-IV in salt-free MES buffer and EDAC/NHS. This indicates that under salt-free, but not physiological, conditions the Debye lengths
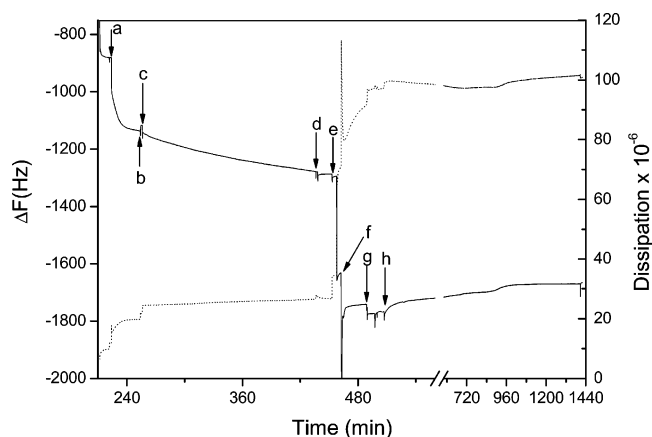
CDV

Figure 7. Frequency (solid line) and dissipation (dashed line) changes during binding of Col-IV and subsequent Matrigel incubation on a LbL film. (a) addition of final HA layer, (b) MES rinse, (c) 5 μg/mL Col-IV in 5 mM MES, EDAC/NHS; (d) MES rinse followed by 50 mM hydroxylamine; (e) MES rinse followed by DMEM; (f) ice-cold DMEM followed by 1:20 Matrigel in DMEM; (g) DMEM rinse; (h) DMEM with 10% FBS.

for the HA and col-IV are large enough for electrostatic interactions to overcome the steric repulsion due to structuring of water by the HA.

Collagen Binding and Matrix Self-Assembly. The activity of the bound collagen layer toward further specific binding was probed using a freshly prepared LbL surface with 4 $^1/_2$ bilayers (Figure 7, see caption for details of solution changes). The change in film thickness due to the adsorption of Col-IV after 2 h was estimated using the Q-Tools software to be approximately 14 nm. After reduction with hydroxylamine to remove any remaining NHS ester from the surface, the film was swelled in DMEM and incubated with 1:20 diluted Matrigel solution in DMEM (mixed on ice and added ice-cold to avoid premature complex formation). The binding of Matrigel led to a relatively small drop in frequency of approximately 140 Hz at the third overtone; however, this was combined with a very large increase in the dissipation signal, indicating the attachment of a layer with relatively high viscosity and low elasticity. Further incubation of the film with 10% FBS in DMEM led to a small loss of mass (approximately 90 Hz change at the third overtone) with relatively little change in dissipation, probably due to enzymatic degradation by the hydrolytic enzymes present in serum.

Film Stability. Stability of the multilayer against serum hyaluronidase was probed by incubating a freshly formed surface with 10% serum in DMEM (Figure 8, see caption for details of solution changes). Upon contact with the serum-containing solution, an increase in frequency and decrease in dissipation was observed, reaching a steady state after approximately 1 h. After correcting for the swelling of the film due to the addition of DMEM, this change corresponded very closely to the frequency drop observed due to the final HA layer. This indicates that the outer HA layer was, indeed, susceptible to hyaluronidase degradation, however the underlying chitosan layer remained essentially impermeable toward serum proteins. The lack of any subsequent increase in film mass appears to indicate that the film retained its nonprotein-adhesive properties. The relatively small loss of mass upon coating with protein (Figure 7) appears to indicate that the cross-link density between the collagen IV and HA was high enough to prevent significant structural disruption by hyaluronidase.

Modulation of Film Stability. One potential approach to increasing the biodegradability of the chitosan component of
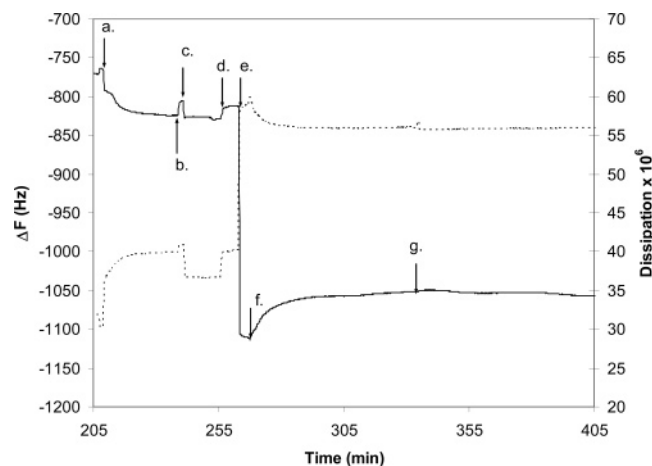

Figure 8. Frequency (solid line) and dissipation (dashed line) during breakdown of a LbL film in 10% serum. (a) addition of final HA layer; (b) MES rinse; (c) 50 mM hydroxylamine; (d) MES rinse; (e) DMEM (f) DMEM + 10% FBS; (g) DMEM
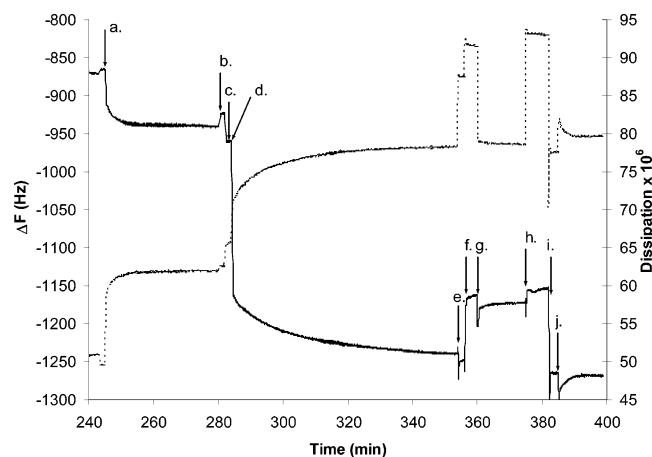

Figure 9. Frequency (solid line) and dissipation (dashed line) changes during acetylation and serum incubation. (a) addition of final HA layer; (b) 5 mM MES rinse; (c) 50 mM MES; (d) 10 mM NaAc, 10X EDAC/NHS; (e) 50 mM MES; (f) 5 mM MES (g) 10 mM AmOH; (h) 5 mM MES; (i) DMEM; (j) DMEM + 10% FBS.

the multilayer film is to acetylate the remaining free amine groups after production of the film, and prior to binding of proteins. As a first attempt at this, a multilayer film was incubated with 10 mM sodium acetate in the presence of 5 mg/mL EDAC and 10 mg/mL NHS (Figure 9, see caption for details of solution changes). As expected, the progression of the acetylation reaction led to a very significant swelling of the film due to the loss of positive charges on the chitosan. In addition, the frequency change upon changing from MES buffer to DMEM (point h − point i) was reduced from approximately 300 Hz to 100 Hz, while the total frequency change from the nonacetylated film in MES (point b) to the final film in DMEM (point i) was approximately 340 Hz, very similar to that for the unmodified multilayer. On addition of 10% serum in DMEM, however, no loss of film mass was observed. A small drop in frequency of less than 10 Hz was observed coupled with an increase in dissipation of approximately 2.5×10^{-6}; however, this effect was completely reversed upon rinsing in fresh DMEM (not shown) and is attributed to the difference in solution properties caused by the presence of serum proteins. The film mass remained stable through a second incubation in fresh 10% serum (not shown). This appears to indicate that some chemical modification of the HA occurred, rendering it resistant to
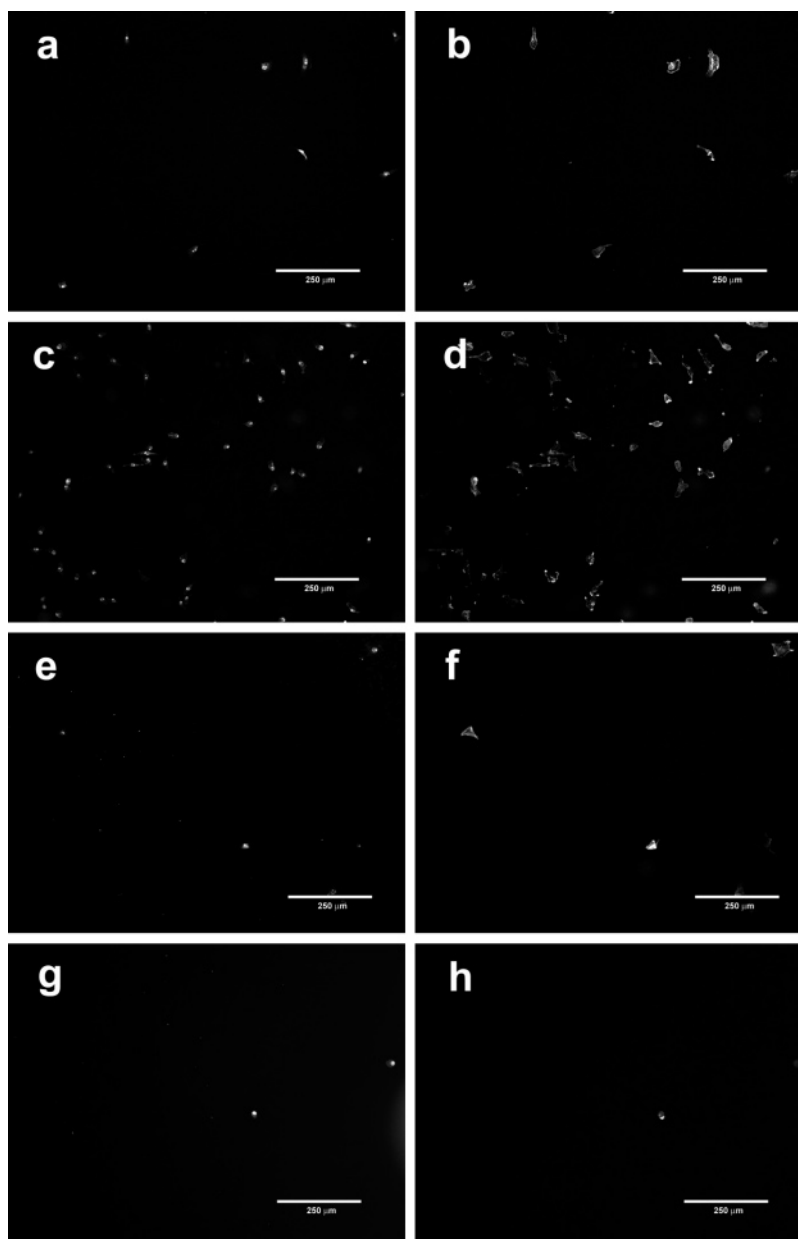
CDV

Figure 10. Fluorescence microscopy images of nuclei (a,c,e,g) and cytoskeletons (b,d,f,h) of NIH-3T3 fibroblasts cultured on untreated (a,b), aminolysed (c,d), hydrolyzed (e,f) and HA-chi 7-layer (g,h) surfaces for 3h. Bar = 250 μm.

hyaluronidase degradation, while retaining its largely nonadhesive properties.

Cell Culture. NIH-3T3 fibroblasts were cultured upon a range of different treated surfaces in 24-well plates for 3 and 48 h, to probe short-term attachment and long-term viability, respectively. Fluorescence images of PO−PRO stained nuclei were obtained from 5 points in each well via a 4× objective (18.6% of total area). Nuclei were counted using particle-counting software (ImageJ, National Institutes of Health).

In the interest of simplicity, cultures of protein-coated multilayer surfaces were carried out using multilayer-coated TCP, rather than PLGA. Bare multilayers on PLGA and TCP showed no statistically significant differences.

Figure 10 compares fluorescence images of cells cultured for 3 h on PLGA-coated coverslips treated via aminolysis with low MW PEI (c, d), hydrolysis with 0.01M NaOH (e, f), or a 7-layer HA-chi multilayer (g, h). Although more cells were attached to the aminolysed surface and less to the hydrolyzed surface

relative to untreated PLGA (a, b), the majority of attached cells on all three surfaces were well spread, with actin filaments and focal adhesion complexes (FAC) becoming apparent. In contrast, on the multilayer surface, the few adherent cells remained rounded, with very little evidence of spreading within any of the viewing fields analyzed.

The behavior of cells on an identical multilayer surface formed on TCP (Figure 11a,b) was indistinguishable from those cultured on multilayer-PLGA. Further binding of collagen IV (c, d) and collagen IV + Matrigel (e, f) essentially reversed this nonadhesive effect, and cytoskeletal organization within cells on these surfaces appeared indistinguishable from cells cultured on TCP (g, h).

After 48 h, cultures on treated PLGA surfaces (Figure 12) displayed some interesting differences. Although cultures on untreated and hydrolyzed PLGA were essentially indistinguishable, forming well-attached, albeit patchy, monolayers, the behaviour on aminolysed PLGA was obviously different. Large clumps of cells were observed, very closely packed and staining
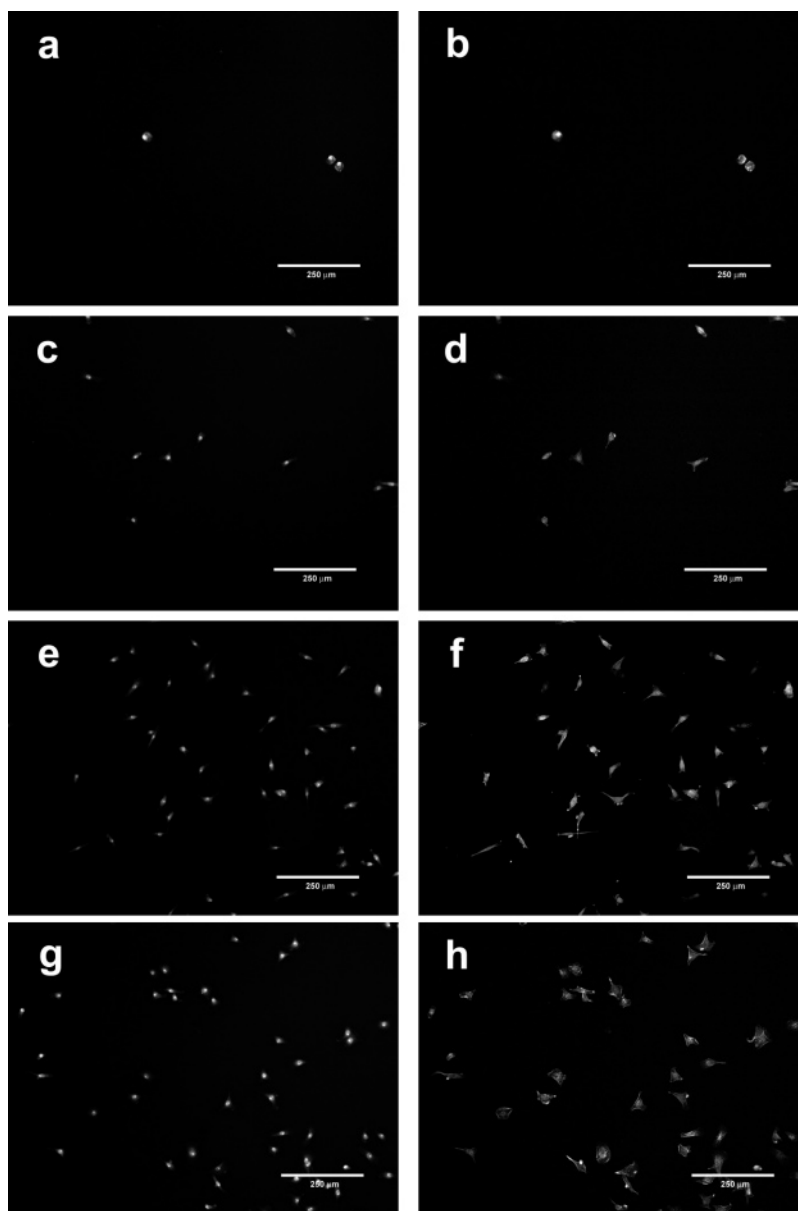
CDV

Figure 11. Fluorescence microscopy images of nuclei (a,c,e,g) and cytoskeletons (b,d,f,h) of NIH-3T3 fibroblasts cultured on tissue culture plastic coated with HA-Chi 7-layer (a,b), 7-layer + col IV (c,d), 7-layer + col IV + Matrigel (e,f) and control (no coating) (g,h) for 3h. Bar = 250 μm.

strongly for actin, often associated with alignment of the cells into bundles. The reason for this behavior remains unclear.

Multilayer-coated surfaces on PLGA (Figure 12g,h and Figure 13a,b) remained essentially nonadhesive after 48 h, with no evidence of cell spreading observed. Cultures on Col IV (Figure 13c,d) and col IV + Matrigel (e, f) coated multilayers showed cell numbers comparable to TCP (g, h), however, with a markedly different phenotype (shown in detail in Figure 14).

To test the viability of cells on the bare multilayer surfaces after 48 h culture, nonadherent cells were gently aspirated and cultured on fresh TCP for 6 h. Fluorescence images of these (Figure 15) showed the cells readily attached and began to spread out from their initial clusters, indicating an absence of any cytotoxic effects from the multilayer surface.

Although physical treatments on PLGA had a strong effect during the initial stages of cell attachment (Figure 16a), with aminolysis and hydrolysis respectively increasing and decreasing attachment over untreated PLGA, the density attained after 48 h (Figure 16b) was essentially identical for all three surfaces.

Note, however, that the apparent phenotype on the aminolysed surface at this point appeared significantly different from that on other surfaces.

Attachment to HA-chi multilayers on TCP and PLGA was statistically similar at both timepoints ($P = 0.2$) and remained extremely low throughout, increasing from 1.2 ± 1 cells/mm^2 after 3 h to 9 ± 7 cells/mm^2 after 48 h. At the latter time-point, however, these were clustered into 2.3 ± 1 spheroids/mm^2, with no evidence of spreading. Nonadherent cells aspirated from the 48h culture and cultured on TCP for 6h showed an adherence rate of 37 ± 15 cells/mm^2; these, plus the cells remaining adhered to the multilayer, account for essentially all the cells originally added (8500 ± 4000/well cf. 10000/well) in the absence of any cell division. Thus, although these surfaces do not support cell growth, they show no evidence of cytotoxicity.

Attachment of col IV with or without added Matrigel restored early cell attachment to significantly higher than untreated PLGA ($P < 0.01$); no significant difference was seen between the two treatments at this point ($P = 0.3$). However, after 48 h, CDV
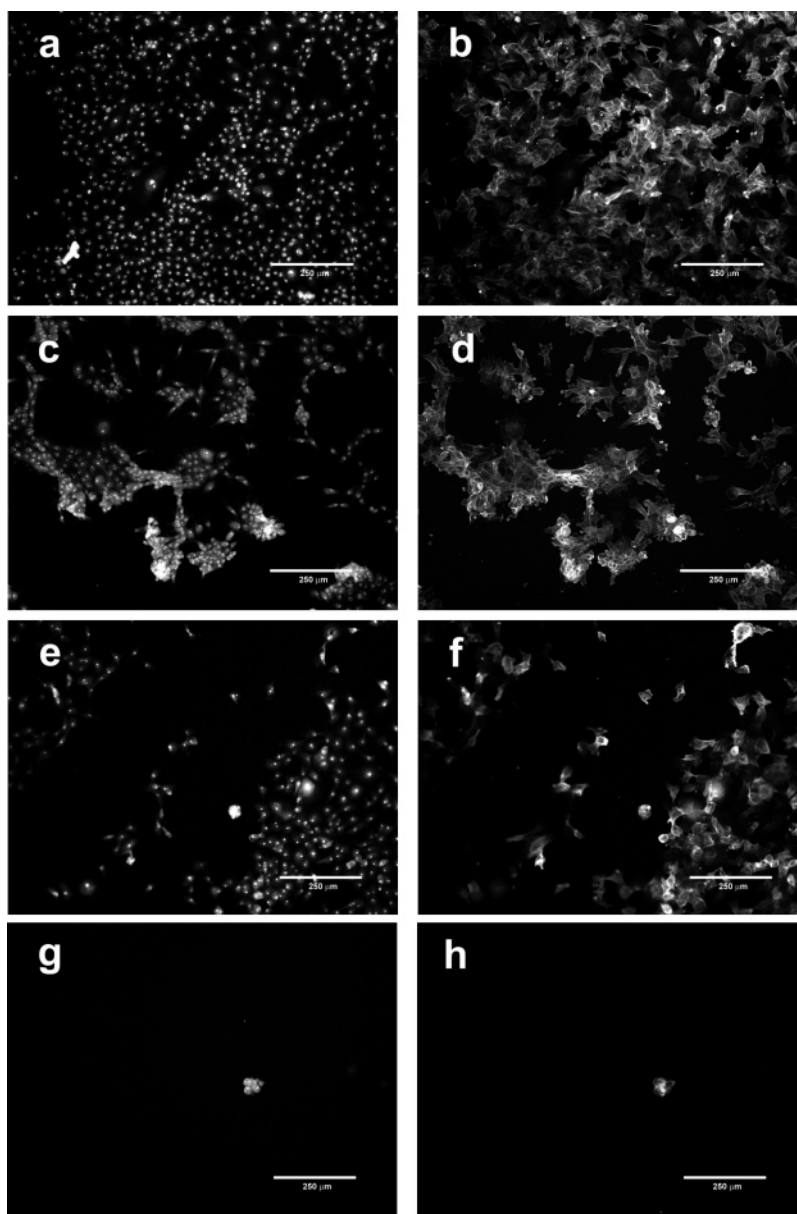
Figure 12. Fluorescence microscopy images of nuclei (a,c,e,g) and cytoskeletons (b,d,f,h) of NIH-3T3 fibroblasts cultured on untreated (a,b), aminolysed (c,d), hydrolyzed (e,f) and HA-chi 7-layer (g,h) surfaces for 48h. Bar = 250 μm.

the col IV + Matrigel surface showed clearly higher growth than either the mutilayer + col IV or untreated PLGA surfaces ($P < 0.01$), and was statistically equivalent to TCP ($P = 0.35$).

Discussion

As the tissue engineering field matures, it is becoming more and more apparent that bio-functionality is of paramount importance in the design of scaffolds. Rather than simply providing empty space for tissue ingrowth as in first-generation scaffolds, it is desirable for the scaffold environment to actively drive and guide the growth of the specific tissue of interest. Rather than a nonspecific, aggressive wound-healing and foreign-body response, it may be hypothesized that a scaffold presenting at its surface ECM proteins from the tissue of interest assembled into their native quarternary structure may stimulate a less aggressive re-modeling response.

The use of layer-by-layer polyelectrolyte deposition to form strong, coherent surface coatings and nanoparticles has been described extensively in the literature.[15−17] Recently, this method

has been adapted for use in tissue engineering applications using various combinations of polyethylenimine, positively and negatively charged gelatin,[18,31] and preliminary studies have been carried out using collagen I and HA.[32]

The biodegradability of the surface modifying polymers is obviously very important. Ideally, the surface should break down gracefully under the action of remodeling enzymes, either into naturally occurring metabolites or into fragments small enough to be excreted through the kidneys (less than approximately 30 Å or 50−70 kDa[33]). The rate of this breakdown should, however, be slow enough that the underlying polymer degrades completely before the surface coating is broken down, to avoid a "discovered" foreign body response. The majority of synthetic polyelectrolytes are, unfortunately, nonbiodegradable, and hence not suitable for this type of tissue engineering application.

Hyaluronic acid (HA) is a strictly alternating copolymer of glucuronic acid and *N*-acetyl-D-glucosamine which is ubiquitous throughout the tissues of the body, generally with molecular weights in the mega-Dalton range.[34−37] Although much remains to be learned about this deceptively simple polymer, it is known
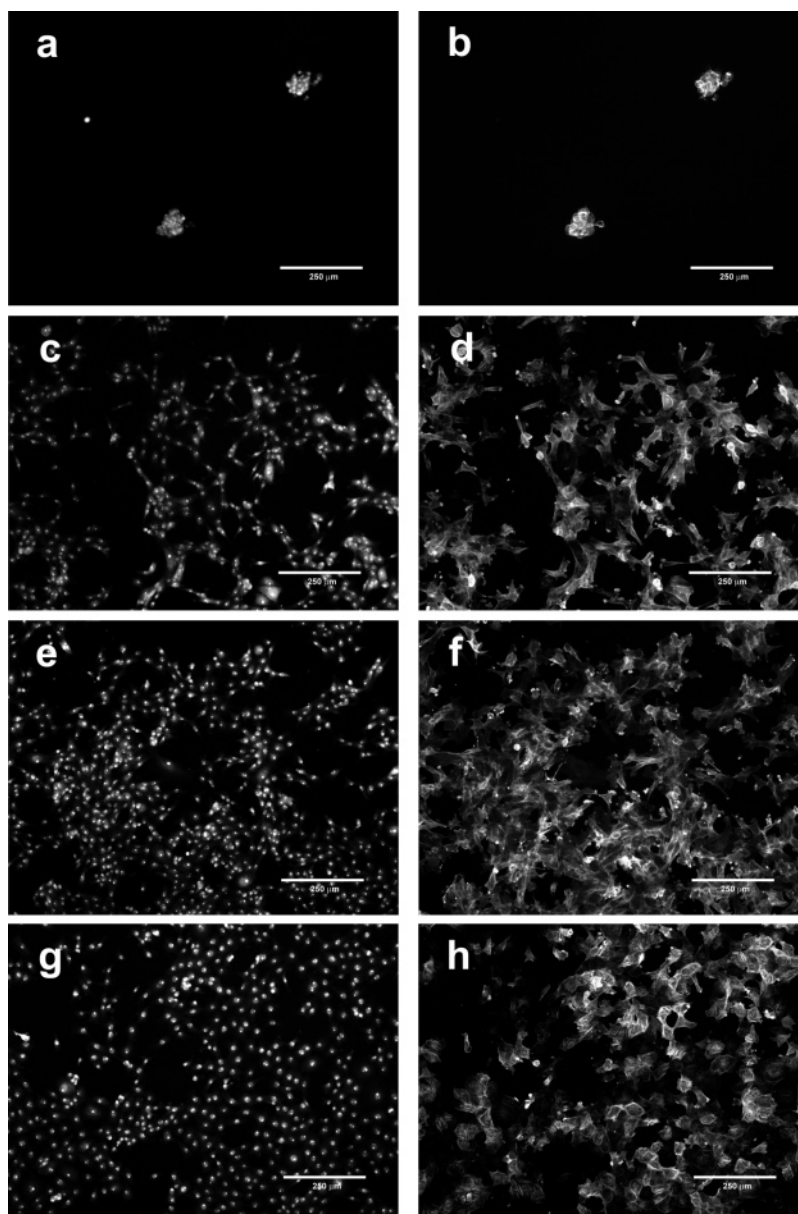
CDV

Figure 13. Fluorescence microscopy images of nuclei (a,c,e,g) and cytoskeletons (b,d,f,h) of NIH-3T3 fibroblasts cultured on tissue culture plastic coated with HA-Chi 7-layer (a,b), 7-layer + col IV (c,d), 7-layer + col IV + Matrigel (e,f) and control (no coating) (g,h) for 48h. Bar = 250 μm.

to be strongly nonadhesive toward most proteins, only binding through specific sites to some epitopes of the CD44 cell surface receptor[38] and to the hyaluronidases. HA thus presents an ideal surface according to the blank slate principle, since the carboxylic acid groups present throughout the chain are readily activated, for example via standard carbodiimide chemistry, to allow the attachment of biologically active molecules. Furthermore, its naturally nonadhesive nature may be expected to lead to minimal denaturation of any bound protein.

Chitosan, a random copolymer of D-glucosamine and N-acetyl-D-glucosamine, is the partially de-acetylated derivative of chitin (poly(N-acetyl-D-glucosamine)), the structural component of the hard shell of insects and crustaceans. Although not naturally present within the human body, it has been found in a number of studies[39,40] to provoke a minimal immune response when implanted in animals.

It has been shown in numerous studies that, although the deacetylated residues in chitosan are essentially nondegradable, the acetylated residues can be broken down slowly under the action of lysozyme, and to a lesser extent by other catabolic enzymes.[40-42] If the resultant fragments are soluble and less than approximately 30 kDa[33] they may then be excreted via the kidneys. Tomihata et al.[40] showed that films of partially deacetylated chitosan implanted in vivo for 12 weeks underwent a sharp transition from <5% polymer remaining to >90% remaining when going from approximately 60% to 70% deacetylation. This behavior can be entirely described using a simple statistical model. The chitosan film is considered as a number of molecular "layers" in which acetylated fragments are considered degradable and deacetylated fragments nondegradable. Furthermore, a molecular weight cutoff (MWCO) is defined at which the nondegradable fragments (continuous homopolymers of deacetylated residues) become insoluble. If the percentage of the surface "blocked" by these nondegradable fragments is calculated as a function of degree of deacetylation through a large number of layers, this behavior is naturally replicated for a MWCO of approximately 2500−3500 Da. These data appear to indicate that either re-acetylation of the chitosan
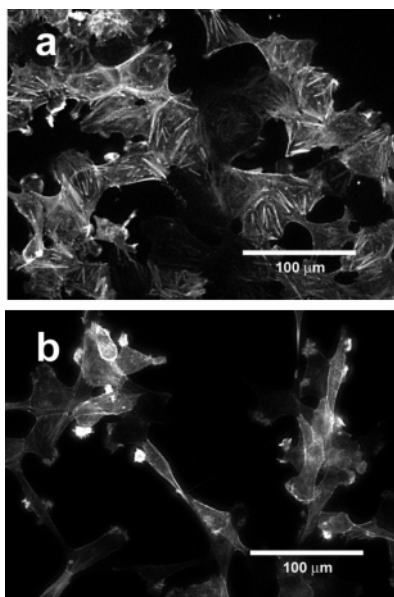
CDV

Figure 14. Comparison of the cytoskeletal organization of NIH-3T3 fibroblasts cultured for 48h on (a) TCP and (b) 7-layer + col IV surfaces. Cells cultured on the multilayer + protein surfaces displayed a markedly different phenotype compared to TCP. Bar = 100 μm.

post-production or use of a stock chitosan with a degree of deacetylation <60% should allow the eventual complete degradation of the multilayer film.

The layer-by-layer buildup of high molecular weight weak polyelectrolytes has been shown previously to be somewhat unstable due to the formation of soluble complexes between the solvated polymer and the previous layer.[29,43] This behavior is seen in the hyaluronic acid-chitosan system described here (Figure 1). Furthermore, upon incubation in a solution at physiological pH, the film dissolves almost entirely due to the deprotonation of the chitosan and subsequent loss of positive charge.

However, preincubation of the hyaluronic acid with EDAC and NHS to promote covalent binding with the primary amine groups on deacetylated chitosan residues changes this behavior significantly (Figure 2), leading to the regular buildup of a film that is highly stable through multiple changes of salt concentration and pH. The changes in the measured vibrational frequency of coated QCM electrodes, and hence the modeled film thickness (Figures 3 and 5 respectively) were found to be approximately linear with respect to layer number after the first few layers, indicating minimal diffusion of polymer chains through the layers.[44] Increasing the polyelectrolyte concentration 10-fold to reflect the higher surface area within a scaffold increased the thickness per layer by approximately 30% and greatly increased the attachment kinetics (Figure 4) but did not appear to otherwise change the film behavior.

The extremely fast deposition kinetics observed (Figure 4) present something of a conundrum. Using a simple transient diffusion model and diffusion coefficients for HA and chitosan reported in the literature[45,46] it can be easily shown that, according to Fick's law, the expected time scale for deposition of a single layer is on the order of hours to days. Thus it would appear that fluid flow is the dominating factor determining adsorption kinetics. Indeed, in most cases, more than 50% of the final mass of each layer deposited during the approximately 20 s of flow required to change solutions.

Upon subjection to challenges with a number of different protein solutions at physiological salt concentration (Figure 6), there was no observable change in the mass of a multilayer

film. However, upon exposure to collagen IV in salt-free buffer, there was a significant increase in film mass. This was coupled to a very significant drop in the dissipation, indicating a contraction of the outer layer due to protein−polymer association and ejection of water.

Incubation of a collagen IV-coated multilayer surface on a QCM electrode with dilute Matrigel (Figure 7) led to a relatively small drop in resonant frequency coupled to a very large increase in dissipation. This is indicative of a relatively soft layer with significant viscous behavior, lending support to the hypothesis of the formation of a protein network extending outward from the surface.

The short-term stability of multilayer surfaces in the presence of hydrolytic enzymes was tested by incubating films with (Figure 7) and without (Figure 8) covalently bound ECM proteins in the presence of 10% fetal bovine serum in DMEM. In the presence of bound protein, a small amount of mass loss was observed, whereas in its absence, a significant amount of mass was lost, apparently corresponding to the mass of the outer HA layer. Thus, it would appear that cross-link density to the bound protein is sufficiently high to prevent significant loss of structure.

The change to a highly hydrolysis-resistant film observed upon treatment with sodium acetate and EDAC/NHS (Figure 9) is likely due to the esterification of the HA via a similar mechanism to that used by Tomihata and Ikada[47] to create cross-linked HA films. They showed that the alcohol groups in HA are nucleophilic enough to esterify with carbodiimide-activated carboxylic acids. This treatment appears to lead to a film that is enzyme-resistant, while still retaining its nonadhesive and, hence, noninteractive properties. It has been shown previously that esters of HA (e.g., Hyaff 48) gradually hydrolyze back to native HA under physiological conditions, thus ensuring their long-term biodegradability. The swelling of the film during this treatment is strong evidence that the amine groups on the chitosan are simultaneously acetylated, rendering the chitosan susceptible to enzymatic degradation.

It is highly likely that the degree of cross-linking will have a significant effect on the long-term biodegradability of these scaffolds; however, this has not yet been tested. Cross-linked saccharide residues are unlikely to break down under enzymatic action and, hence, present a barrier to complete elimination. As long as the resultant fragments are smaller than approximately 30 kDa, however, complete elimination via the kidneys is theoretically possible. The effect of the cross-link density on the degradation of the coating will be probed in later studies.

Of course, the ultimate test of any surface modification is its performance under cell culture conditions. To this end, NIH-3T3 fibroblasts were cultured with a range of different surface treatments. NIH-3T3 cells, like many fibroblasts, express a wide range of integrins and other surface adhesion proteins and therefore make a good probe for the presence of unidentified bound proteins.

Although simple surface modification via hydrolysis or aminolysis made a difference to the cell response during the early attachment phase (Figures 10a−f and 15a), there was no difference in cell numbers after 48 h (Figure 16b), although the cell phenotype on the aminolysed surface appeared somewhat different (Figure 12c,d). Thus, the effects of these modifications appear to be relatively subtle and short-lived.

In contrast, the effect of the multilayer coating on cell behavior, either on PLGA (Figures 10g,h and 12g,h) or TCP (Figures 11a,b and 13a,b), was profound. Very few cells attached
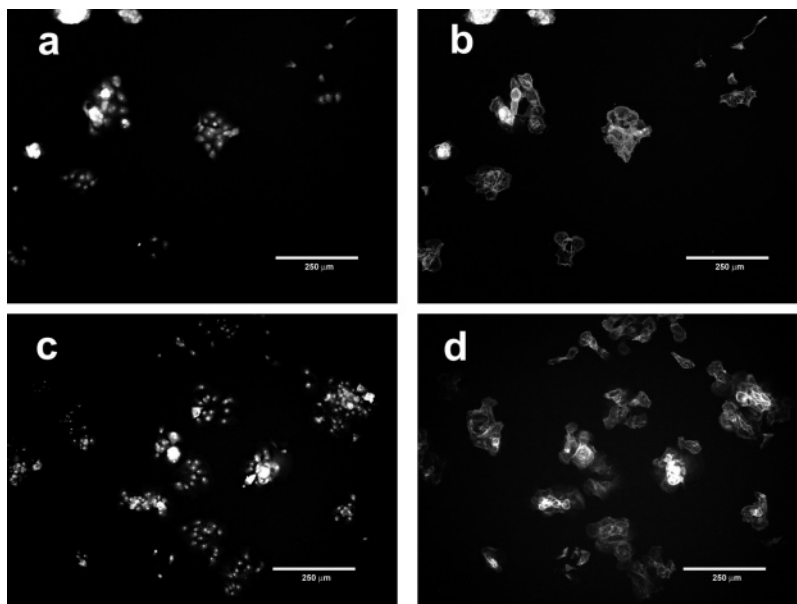
CDV

Figure 15. Fluorescence microscopy images of nuclei (a,c) and cytoskeletons (b,d) of NIH-3T3 fibroblasts aspirated from 48h cultures on (a,b) HA-chi 7 PLGA or (c,d) HA-chi 7 TCP and cultured for 6h on fresh TCP. Bar = 250 μm.
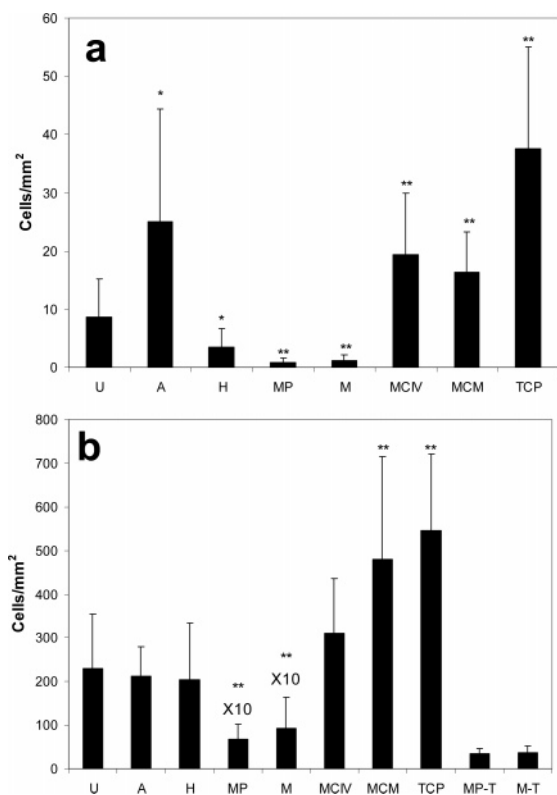

Figure 16. Cell attachment density as determined by counting of fluorescently tagged nuclei after 3h (a) and 48h (b) of culture in a 24-well plate (10^4/well inoculum). Five areas were imaged (6.56 mm^2/image) on each of 3 (PLGA substrate) or 4 (TCP substrate) wells. Presented data is mean ± standard deviation. U = untreated PLGA, A = aminolysed, H = hydrolyzed, MP = multilayer on PLGA, M = multilayer on TCP, MCIV = multilayer + col IV, MCM = multilayer + col IV + Matrigel, TCP = tissue culture polystyrene, MP-T and M−T = cells aspirated off MP and M respectively and cultured on TCP for 6h. Symbols * and ** refer to t-statistic values less than 0.05 and 0.01 respectively relative to untreated PLGA. × 10 above a bar indicates that the values have been multiplied by a factor of 10 for the sake of visibility.

(Figure 16) and those that did remained rounded and clumped throughout the experiment. The viability of the nonadherent cells

at 48 h appeared uncompromised when transferred back to TCP (Figure 15), indicating that this nonadherence was not due to a cytotoxic effect. At this stage, these surfaces appear promising as a potential new noninteractive coating for invasive medical devices such as catheters and may also be useful for the culture of naturally nonadherent cells such as chondrocytes.

Upon the addition of collagen IV, and subsequently Matrigel, to this surface, however, cell numbers (Figure 16) were restored to levels comparable to TCP, however with a somewhat different morphology (Figures 11b−f, 13b−f, and 14). This evidence suggests that in this case, the cell attachment was mediated entirely either directly via the collagen IV and Matrigel components or via serum proteins bound to these proteins through specific interactions. Thus, it appears likely that these surfaces may be considered a step closer to the goal of precision control of cell response in vitro and potentially in vivo.

Conclusions

In this paper, we have demonstrated the formation of a highly engineered surface for tissue engineering applications, entirely from materials that are either fully biodegradable, or degradable to fragments small enough to be excreted.

Two-dimensional studies in the quartz crystal microbalance (QCM) showed that the presence of a cross-linking agent such as 1-ethyl-3-(3-dimethylaminopropyl)-carbodiimide (EDAC) is necessary to ensure stability during the buildup process under these conditions. It was further shown that the resulting films are nonadhesive toward most proteins under physiological conditions while incorporating functional groups allowing the easy attachment of suitable proteins such as collagen IV under salt-free conditions. Additionally, it was demonstrated that the stability of these films against enzymatic degradation can be modulated while retaining their nonadhesive properties.

Using NIH-3T3 fibroblasts, we showed that the multilayer coating almost completely negates cell attachment and spreading in serum-containing medium, which can then be reinstated to levels similar to tissue culture polystyrene upon attachment of collagen IV.

Since hyaluronic acid is essentially ubiquitous within the human body, the HA/chitosan multilayer surface described here

CDV

can be thought of as a potential "generic" surface treatment. By varying the choice of scaffold morphology, base polymer, protein attachment, and growth factor incorporation, scaffolds made using this technique could potentially be adapted for use in most, if not all, tissue engineering applications currently under investigation.

References and Notes

(1) Cao, Y.; Davidson, M. R.; O'Conner, A. J.; Stevens, G. W.; Cooper-White, J. J. Architecture control of three-dimensional polymeric scaffolds for soft tissue engineering i. Establishment and validation of numerical models. *J. Biomed. Mater. Res.* **2004**, *71A*, 81−89.

(2) Cao, Y.; Croll, T. I.; O'Connor, A. J.; Stevens, G. W.; Cooper-White, J. J. Systematic selection of solvents for the fabrication of 3D combined macro- and microporous polymeric scaffolds for soft tissue engineering. *J. Biomater. Sci.-Polym. Ed.* **2006**, in press.

(3) Nam, Y. S.; Park, T. G. Porous biodegradable polymeric scaffolds prepared by thermally induced phase separation. *J. Biomed. Mater. Research* **1999**, *47*, 8−17.

(4) Shen, M. C.; Garcia, I.; Maier, R. V.; Horbett, T. A. Effects of adsorbed proteins and surface chemistry on foreign body giant cell formation, tumor necrosis factor alpha release and procoagulant activity of monocytes. *J. Biomed. Mater. Res. Part A* **2004**, *70A* (4), 533−541.

(5) Kao, W. J.; Hubbell, J. A.; Anderson, J. M. Protein-mediated macrophage adhesion and activation on biomaterials: a model for modulating cell behavior. *J. Mater. Sci.-Mater. Med.* **1999**, *10* (10−11), 601−605.

(6) Anderson, J. M.; Defife, K.; Mcnally, A.; Collier, T.; Jenney, C. Monocyte, macrophage and foreign body giant cell interactions with molecularly engineered surfaces. *J. Mater. Sci.-Mater. Med.* **1999**, *10* (10−11), 579−588.

(7) Nitschke, M.; Schmack, G.; Janke, A.; Simon, F.; Pleul, D.; Werner, C. Low-pressure plasma treatment of poly(3-hydroxybutyrate): Toward tailored polymer surfaces for tissue engineering scaffolds. *J. Biomed. Mater. Res.* **2002**, *59*, 632−638.

(8) Quirk, R. A.; Davies, M. C.; Tendler, S. J. B.; Shakesheff, K. M. Surface Engineering of Poly(lactic acid) by Entrapment of Modifying Species. *Macromolecules* **2000**, *33*, 258−260.

(9) Dai, L.; StJohn, H. A. W.; Bi, J.; Zientek, P.; Chatelier, R. C.; Griesser, H. J. Biomedical coatings by the covalent immobilization of polysaccharides onto gas-plasma-activated polymer surfaces. *Surf. Interface Anal.* **2000**, *29*, 46−55.

(10) Chu, P. K.; Chen, J. Y.; Wang, L. P.; Huang, N. Plasma-surface modification of biomaterials. *Mater. Sci. Eng. R* **2002**, *36*, 143−206.

(11) Yang, J.; Shi, G.; Bei, J.; Wang, S.; Cao, Y.; Shang, Q.; Yang, G.; Wang, W. Fabrication and surface modification of macroporous poly(L-lactic acid) and poly(L-lactic-*co*-glycolic acid) (70/30) cell scaffolds for human skin fibroblast cell culture. *J. Biomed. Mater. Res.* **2002**, *62*, 438−446.

(12) Zhu, H.; Ji, J.; Lin, R.; Gao, C.; Feng, L.; Shen, J. Surface engineering of poly(D, L-lactic acid) by entrapment of chitosan-based derivatives for the promotion of chondrogenesis. *J. Biomed. Mater. Res.* **2002**, *62*, 532−539.

(13) Quirk, R. A.; Davies, M. C.; Tendler, S. J. B.; Chan, W. C.; Shakesheff, K. M. Controlling Biological Interactions with Poly(lactic acid) by Surface Entrapment Modification. *Langmuir* **2001**, *17*, 2817−2820.

(14) Zhu, H. G.; Ji, J.; Shen, J. C. Surface engineering of poly(DL-lactic acid) by entrapment of biomacromolecules. *Macromol. Rapid Commun.* **2002**, *23* (14), 819−823.

(15) Berg, M. C.; Yang, S. Y.; Hammond, P. T.; Rubner, M. F. Controlling Mammalian Cell Interactions on Patterned Polyelectrolyte Multilayer Surfaces. *Langmuir* **2004**, *20*, 1362−1368.

(16) Tan, H. L.; McMurdo, M. J.; Pan, G.; Van Patten, P. G. Temperature Dependence of Polyelectrolyte Multilayer Assembly. *Langmuir* **2003**, *19*, 9311−9314.

(17) Thierry, B.; Winnik, F. M.; Merhi, Y.; Tabrizian, M. Nanocoatings onto Arteries via Layer-by-Layer Deposition: Toward the in Vivo Repair of Damaged Blood Vessels. *J. Am. Chem. Soc.* **2003**, *125*, 7494−7495.

(18) Zhu, H.; Ji, J.; Shen, J. Construction of multilayer coating onto poly(DL-lactide) to promote cytocompatibility. *Biomaterials* **2004**, *25*, 109−117.

(19) Awodi, Y. W.; Johnson, A.; Peters, R. H.; Popoola, A. V. The aminolysis of poly(ethylene terephthalate). *J. Appl. Polym. Sci.* **1987**, *33* (7), 2503−12.

(20) Collins, M. J.; Zeronian, S. H.; Marshall, M. L. Analysis of the Molecular-Weight Distributions of Aminolyzed Poly(Ethylene-Terephthalate) by Using Gel-Permeation Chromatography. *J. Macromol. Sci.-Chem.* **1991**, *A28* (8), 775−792.

(21) Ellison, M. S.; Fisher, L. D.; Alger, K. W.; Zeronian, S. H. Physical properties of polyester fibers degraded by aminolysis and by alkaline hydrolysis. *J. Appl. Polym. Sci.* **1982**, *27* (1), 247−57.

(22) Croll, T. I.; O'Connor, A. J.; Stevens, G. W.; Cooper-White, J. J. Controllable surface modification of poly(lactic-*co*-glycolic acid) (PLGA) by hydrolysis or aminolysis I: physical, chemical and theoretical aspects. *Biomacromolecules* **2004**, *5* (2), 463−473.

(23) Zhu, Y.; Gao, C.; Liu, X.; Shen, J. Surface modification of polycaprolactone membrane via aminolysis and biomacromolecule immobilization for promoting cytocompatibility of human endothelial cells. *Biomacromolecules* **2002**, *3*, 1312−1319.

(24) Kingshott, P.; McArthur, S.; Thissen, H.; Castner, D. G.; Griesser, H. J. Ultrasensitive probing of the protein resistance of PEG surfaces by secondary ion mass spectrometry. *Biomaterials* **2002**, *23* (24), 4775−4785.

(25) Irvine, D. J.; Mayes, A. M.; Satija, S. K.; Barker, J. G.; Sofia-Allgor, S. J.; Griffith, L. G. Comparison of tethered star and linear poly(ethylene oxide) for control of biomaterials surface properties. *J. Biomed. Mater. Res.* **1998**, *40* (3), 498−509.

(26) Kingshott, P.; Thissen, H.; Griesser, H. J. Effects of cloud-point grafting, chain length, and density of PEG layers on competitive adsorption of ocular proteins. *Biomaterials* **2002**, *23* (9), 2043−2056.

(27) Marx, K. A. Quartz crystal microbalance: A useful tool for studying thin polymer films and complex biomolecular systems at the solution-surface interface. *Biomacromolecules* **2003**, *4* (5), 1099−1120.

(28) Zhou, C.; Friedt, J. M.; Angelova, A.; Choi, K. H.; Laureyn, W.; Frederix, F.; Francis, L. A.; Campitelli, A.; Engelborghs, Y.; Borghs, G. Human immunoglobulin adsorption investigated by means of quartz crystal microbalance dissipation, atomic force microscopy, surface acoustic wave, and surface plasmon resonance techniques. *Langmuir* **2004**, *20* (14), 5870−5878.

(29) Kovacevic, D.; van der Burgh, S.; de Keizer, A.; Cohen Stuart, M. A. Kinetics of Formation and Dissolution of Weak Polyelectrolyte Multilayers: Role of Salt and Free Polyions. *Langmuir* **2002**, *18*, 5607−5612.

(30) Voinova, M. V.; Rodahl, M.; Jonson, M.; Kasemo, B. Viscoelastic acoustic response of layered polymer films at fluid-solid interfaces: continuum mechanics approach. *Phys. Scripta* **1999**, *59*, 391−396.

(31) Zhu, H. G.; Ji, J.; Barbosa, M. A.; Shen, J. C. Protein electrostatic self-assembly on poly(DL-Lactide) scaffold to promote osteoblast growth. *J. Biomed. Mater. Res. Part B-Appl. Biomater.* **2004**, *71B* (1), 159−165.

(32) Zhang, J.; Senger, B.; Vautier, D.; Picart, C.; Schaaf, P.; Voegel, J. C.; Lavalle, P. Natural polyelectrolyte films based on layer-by layer deposition of collagen and hyaluronic acid. *Biomaterials* **2005**, *26* (16), 3353−3361.

(33) Grieve, K. A.; Nikolic-Paterson, D. J.; Guimarães, M.A. M.; Nikolovski, J.; Pratt, L. M.; Mu, W.; Atkins, R. C.; Comper, W. D. Glomerular permselectivity factors are not responsible for the increase in fractional clearance of albumin in rat glomerulonephritis. *Am. J. Pathol.* **2001**, *159* (3), 1159−1170.

(34) Kakehi, K.; Kinoshita, M.; Yasueda, S.-i. Hyaluronic acid: separation and biological implications. *J. Chromatogr. B* **2003**, *797*, 347−355.

(35) Noble, P. Hyaluronan and its catabolic products in tissue injury and repair. *Matrix Biol.* **2002**, *21*, 25−29.

CDV

(36) Tammi, M. I.; Day, A. J.; Turley, E. A. Hyaluronan and Homeostasis: A Balancing Act. *J. Biol. Chem.* **2002**, *277* (7), 4581−4584.

(37) Termeer, C.; Sleeman, J. P.; Simon, J. C. Hyaluronan − magic glue for the regulation of the immune response? *Trends Immunol.* **2003**, *24* (3), 112−114.

(38) Isacke, C. M.; Yarwood, H. The hyaluronan receptor, CD44. *Int. J. Biochem. Cell Biol.* **2002**, *34*, 718−721.

(39) Rao, S. B.; Sharma, C. P. Use of chitosan as a biomaterial: Studies on its safety and hemostatic potential. *J. Biomed. Mater. Res.* **1997**, *34* (1), 21−28.

(40) Tomihata, K.; Ikada, Y. In vitro and in vivo degradation of films of chitin and its deacetylated derivatives. *Biomaterials* **1997**, *18*, 8 (7), 567−575.

(41) Muzzarelli, R. A. A.; Mattioli-Belmonte, M.; Miliani, M.; Muzzarelli, C.; Gabbanelli, F.; Biagini, G. In vivo and in vitro biodegradation of oxychitin-chitosan and oxypullulan-chitosan complexes. *Carbohydr. Polym.* **2002**, *48* (1), 15−21.

(42) Serizawa, T.; Yamaguchi, M.; Akashi, M. Enzymatic Hydrolysis of a Layer-by-Layer Assembly Prepared from Chitosan and Dextran Sulfate. *Macromolecules* **2002**, *35*, 8656−8658.

(43) Kovacevic, D.; van der Burgh, S.; de Keizer, A.; Cohen Stuart, M. A. Specific Ionic Effects on Weak Polyelectrolyte Multilayer Formation. *J. Phys. Chem. B* **2003**, *107*, 7998−8002.

(44) Schönhoff, M. Layered polyelectrolyte complexes: physics of formation and molecular properties. *J. Phys.: Condensed Matter* **2003**, *15*, R1781−R1808.

(45) Tsaih, M. L.; Chen, R. H. Effects of ionic strength and pH on the diffusion coefficients and conformation of chitosans molecule in solution. *J. Appl. Polym. Sci.* **1999**, *73*, 2041−2050.

(46) Barry, S. I.; Gowman, L. M.; Ethier, C. R. Obtaining the concentration-dependent diffusion coefficient from ultrafiltration experiments: application to hyaluronate. *Biopolymers* **1996**, *39*, 1−11.

(47) Tomihata, K.; Ikada, Y. Cross-linking of hyaluronic acid with water-soluble carbodiimide. *J. Biomed. Mater. Res.* **1997**, *37*, 243−251.

(48) Halbleib, M.; Skurk, T.; de Luca, C.; von Heimburg, D.; Hauner, H. Tissue engineering of white adipose tissue using hyaluronic acid-based scaffolds. I: in vitro differentiation of human adipocyte precursor cells on scaffolds. *Biomaterials* **2003**, *24* (18), 3125−3132.